Heliyon 6 (2020) e05711

Contents lists available at ScienceDirect

Heliyon

journal homepage: www.cell.com/heliyon

Research article

Characteristics of laser induced breakdown investigated by a compact, nongated optical multichannel analyzer system and its potential application

Nasrullah Idris [a,*], Kurnia Lahna [a], Muliadi Ramli [b], Taufik Fuadi Abidin [c], Wahyu Setia Budi [d], Maria Margareta Suliyanti [e], Koo Hendrik Kurniawan [f], May On Tjia [f,g], Kiichiro Kagawa [f,h]

[a] Department of Physics, Faculty of Mathematics and Natural Sciences, Syiah Kuala University, Darussalam, Banda Aceh, 23111, Aceh, Indonesia
[b] Department of Chemistry, Faculty of Mathematics and Natural Sciences, Syiah Kuala University, Darussalam, Banda Aceh, 23111, Aceh, Indonesia
[c] Department of Informatics, Faculty of Mathematics and Natural Sciences, Syiah Kuala University, Darussalam, Banda Aceh, 23111, Aceh, Indonesia
[d] Department of Physics, Faculty of Mathematics and Natural Sciences, Diponegoro University, Tembalang, Semarang, 50275, Indonesia
[e] Research Center for Physics, Indonesia Institute of Sciences, Kawasan PUSPIPTEK, Serpong, Tangerang Selatan, 15314, Banten, Indonesia
[f] Research Center of Maju Makmur Mandiri Foundation, 40 Srengseng Raya, Kembangan, Jakarta Barat, 11630, Indonesia
[g] Physics of Magnetism and Photonics Group, Faculty of Mathematics and Natural Sciences, Bandung Institute of Technology, 10 Ganesha, Bandung, 40132, Indonesia
[h] Fukui Science Education Academy, Takagi Chuo 2 chome, Fukui, 910-0804, Japan

ARTICLE INFO

Keywords:
Analytical chemistry
Optics
Plasma physics
Laser induced breakdown spectroscopy
Compact OMA system
Plasma characteristics
Jewelry sample
Stone sample

ABSTRACT

Laser induced breakdown is a highly temporally and spatially dynamic phenomenon, normally studied using a highly temporally resolved optical detector system. In this work, a compact, low cost optical multichannel analyzer (OMA) system without a built-in temporal gating device and thus operated under a free running mode was used to investigate the characteristics of laser induced plasma. A Nd-YAG laser beam was used as the excitation source from several samples, namely, copper, zinc, and aluminum plates. The characteristics of the plasma emission produced under various experimental parameters, including the pulse energy, surrounding gas pressure, and collection fiber position, were examined. It was found that the essential features of emission spectra can be investigated even using the ungated, compact OMA system even without a highly temporally resolved gating system. The plasma emission characteristics critically depend on the experimental parameters. A quality emission spectrum, featuring a high intensity with a low background, can be obtained using the ungated, compact OMA system under optimized conditions, namely, a pulse energy of approximately 8 mJ, a surrounding gas pressure of 10 Torr, and a collection fiber position of more than 5 mm above the surface of the sample. The features of the emission spectra detected under optimized conditions are only similar to those obtained using a sophisticated, gated OMA system. The characteristics of the emission spectra are in good agreement with the previous assumption of the shockwave role in plasma excitation. Having quality emission spectra under the optimized conditions, a preliminary practical laser induced breakdown spectroscopy (LIBS) analysis using the ungated, compact OMA system was performed on several samples, such as standard brass, commercial pure gold, and natural stone samples. The aluminum emission lines are strongly detected from the standard brass sample (C1118) containing aluminum at 2.8%. The LIBS system also unequivocally revealed a qualitatively abandoned impurity presence in the purportedly pure commercial gold sample. It also effectively confirmed qualitatively a Cu presence in the blinking spots of the natural stone collected from a traditional mining site in Aceh. This result implies the effectiveness of the LIBS using the ungated, compact OMA system for quick, practical analysis.

1. Introduction

Laser induced breakdown spectroscopy (LIBS) as a new analytical technique now enjoys very high interest and popularity. As an emerging analytical tool, it is considered a new superstar [1]. This is because LIBS has demonstrated many advantages over the conventional analytical techniques. LIBS has a powerful capability for performing direct analysis of different types of samples, including metals and nonmetals in any form of solid, liquid, and gas. The unique advantages of LIBS exclusively important for analysis of difficult samples are nondestructive or virtually

* Corresponding author.
E-mail address: nasrullah.idris@unsyiah.ac.id (N. Idris).

https://doi.org/10.1016/j.heliyon.2020.e05711
Received 26 June 2020; Received in revised form 28 September 2020; Accepted 9 December 2020

nondestructive testing without tedious sample preparation, environmentally friendly sample pretreatments, a simple experimental procedure and equipment arrangement, and very flexible analysis. The analysis can be conducted directly in the ablation site without requiring transportation of the ablated sample into another site for excitation. Moreover, the paramount advantage of LIBS is the capability for simultaneous multielemental analysis over a wide range of wavelengths [2, 3]. This capability is very useful for studying plasma characteristics by observing simultaneously the emission dynamics of many emission spectral lines from various constituents of a sample. The wide-ranging wavelength coverage is also very useful for identifying samples, especially those of complex matrices, such as environmental and geological samples. In fact, LIBS with a high spectral resolution OMA system can reveal complicated emission spectra from environmental and geological samples [4, 5, 6, 7, 8, 9, 10, 11, 12].

Not only driven by the powerful analytical performance over very wide area of applications, the fruitful development of laser induced breakdown spectroscopy research is also largely due to the availability of high quality laser sources and sophisticated optical detectors. The sophisticated OMA system equipped with a highly resolved gating device allows a detailed observation of plasma formation processes and dynamics. This observation leads to a better understanding of plasma characteristics, opening new opportunities for improving the analytical performance and revealing new applications of LIBS in various fields. However, the fast development of LIBS research is witnessed mostly in developed countries, whereas conducting LIBS research in developing countries in limited conditions of research budget and instrumentation is difficult.

In addition to its research purpose, the LIBS experiment is apparently very useful for teaching physics, because it can be used to demonstrate directly many important, abstract concepts in physics, especially those regarding atomic physics and optics. This technique is considered a potential tool for increasing student interest and understanding of physics. Therefore, it is very important to perform LIBS research even under limited conditions in developing countries. Indeed, the first step for starting LIBS research is to obtain a laser, but there is another crucial instrument that is needed for detecting emission spectra, namely, an optical multichannel analyzer (OMA) system. However, a gated, sophisticated OMA system using an intensified charge coupled device remains very expensive. On the other hand, because of recent advances in optical detection science and technology, a compact OMA system with a relatively high spectral resolution spectrograph is now commercially available at an affordable cost. Unfortunately, most of the compact OMA systems are not equipped with a built-in gating device, hindering the acquisition of highly time-resolved emission spectra. This circumstance makes it difficult to perform a LIBS analysis using the ungated, compact OMA system in such a limited condition. Although it does not have a gating system, the compact OMA system has a wide wavelength coverage that promises very useful applications for the characterization, identification, and classification of various samples [4, 5, 6, 7, 8, 9, 10]. To date, the LIBS studies using a compact OMA system have mostly addressed practical applications [13, 14, 15]. The most important and growing application of LIBS using the compact OMA system in LIBS is for stand-off analysis [16, 17].

On the other hand, the wide wavelength coverage of the ungated, compact OMA system also promises the possibility for studying the characteristics and emission dynamics of many elements in the samples of interest. The physical characteristics of laser induced plasma, such as the emission spectra profile, electron number density, and plasma temperature, determine the LIBS analytical performance. Moreover, the experimental parameters, including the pressure of the ambient gas, energy of the laser pulse, and probing position of the collection optical fiber, strongly influence the analytical performance of LIBS [18, 19, 20, 21]. Thus, a better understanding of the plasma characteristics is essential for assuring a better LIBS reliability and effectiveness. Because a sophisticated OMA system equipped with a high spectral resolution spectrograph and a highly temporal resolved gating function remains very expensive considering the limited research budgets and instrumentation in developing countries, it is very important to study the plasma characteristics using the compact OMA system without using any gating function under various experimental parameters and search for the optimum condition allowing for practical qualitative and quantitative analysis to be performed. The capability for conducting LIBS research even using the compact, low cost OMA system is very important because of the wide open area of application in developing countries, especially for practical applications ranging from environmental to geological samples. This situation partly drives the development of a simple, low cost LIBS system [22, 23, 24, 25]. It is well known that the lower environmental standards and weaker law enforcement in developing countries poses a very high risk of hazard to the environment from anthropogenic causes. On the other hand, many developing countries have a vast wealth of natural resources, including minerals and natural precious stones. Aceh is a region in Indonesia that has abundant natural resources, including minerals and gemstones. It is well known that LIBS is

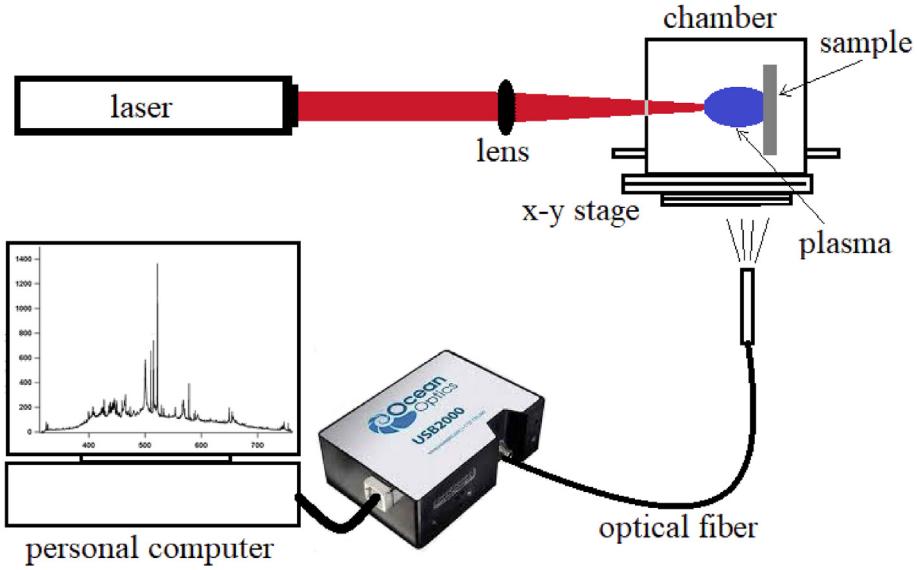

Figure 1. LIBS apparatus arrangement used in this work.

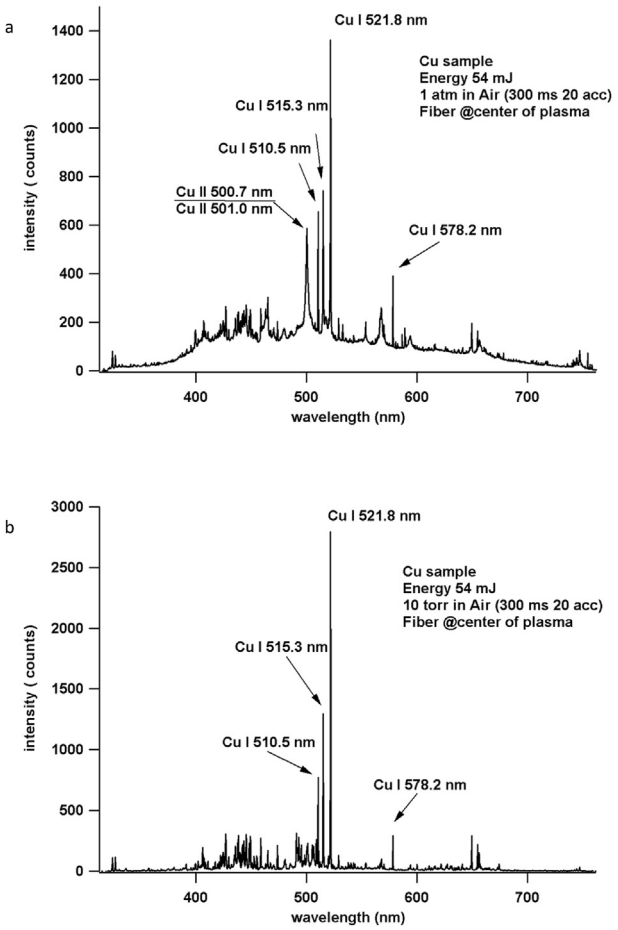

Figure 2. Emission spectrum taken from plasma produced on a pure copper plate using a 54 mJ pulse energy under ambient air at a pressure of (a) 760 Torr and (b) 10 Torr.

a very powerful analytical technique for analyzing complex samples, such as environmental and geological samples. Therefore, it is very important to conduct LIBS research in developing countries even if only a compact, low cost OMA system is used, because of the many potential practical applications ranging from environmental monitoring to analyzing local geological samples. Therefore, in this work, an ungated, compact OMA system was used to evaluate the characteristics of plasma, and its potential for practical applications, particularly in the analysis of various local samples, was examined.

2. Experimental procedures

The LIBS apparatus used in this work is displayed in Figure 1. The main apparatus of this present LIBS setup consists of a neodymium yttrium aluminum garnet (Nd-YAG) laser and a compact OMA system. The Nd-YAG laser operates at a fundamental wavelength of 1064 nm with a repetition rate of 10 Hz. The energy and the duration of the laser pulse are 400 mJ and 8 ns, respectively. The laser beam was focused onto the surface of the sample using a lens (f = +150 mm) under ambient air. The sample was placed in a metal chamber fixed on a movable x-y stage. The metal chamber can be evacuated and filled with a different gas at the desired pressures using a vacuum pump. The plasma emission was collected using a probing optical fiber set on one side of the plasma perpendicular to the laser beam path. The plasma emission collected by the fiber was then delivered to the compact OMA system. The probing optical fiber was fixed on a movable x stage, allowing for moving the fiber precisely along the x-axis perpendicular to the surface of the sample. The OMA system consists of a high resolution spectrograph with a wide wavelength coverage, ranging from the ultraviolet (UV) to visible (VIS) regions, namely, from 350 nm to 750 nm (HR 2000, Ocean optics). The optical resolution of the OMA system is ~0.065 nm (FWHM). This compact OMA system uses a high-sensitivity 2048 element charge couple device array without a gating device. The plasma emission spectra acquisition was performed in the free running mode without any temporal gating function. To acquire an emission spectrum, the integration time and accumulation number of the detector were set for 30 ms and 20 times, respectively. The OMA system was computer operated and controlled using Spectrasuite software.

The influence of several experimental parameters and configuration on the emission spectra was examined. The energy of the laser pulse was varied gradually from 8 mJ to 70 mJ during the experiment. Similarly, the pressure of the ambient air was changed gradually from 5 Torr to 760 Torr. The influence of the probing position of the optical fiber at the plasma on the emission spectra was also studied by precisely moving the fiber position from the position slightly above the sample surface (0 mm) to positions away from the sample surface. The effect of the variation of the experimental parameters and configuration on the characteristics of the produced plasma was examined in terms of the appearance atomic and ionic spectral lines and their intensities, the intensity of background emission, plasma temperature, energy dependence profile, pressure dependence profile and fiber probing position influence. Pure metal samples, including copper, zinc, and aluminum plates, were used in this work. To quickly examine the performance of LIBS using the compact, ungated OMA system, a standard brass sample (C1118, Rare Metallic Corporation, Japan) with specified elemental concentrations was used. In addition, a pure gold sample purchased commercially was also used. LIBS using the compact, ungated OMA system was used to analyze quickly natural stone collected from Aceh, Indonesia.

3. Experimental results and discussion

Figure 2(a) displays the emission spectrum obtained from plasma produced on the pure copper plate using the compact OMA system and a pulse energy of 54 mJ under ambient air at a pressure of 760 Torr. The pulse energy corresponds to a fluency of 27.52 J/cm^2 in our experiment. The optical fiber for collecting the plasma emission was probed just on the center of the plasma at a position approximately 5 mm from the surface of the sample. A strong emission spectrum with a very high background level is clearly shown. The emission spectrum is mostly dominated by copper emission lines. The copper emission lines, including typical atomic emission lines in visible regions (Cu I 510.5 nm, Cu I 515.3 nm, and Cu I 521.8 nm) and Cu I 578.2 nm together with ionic emission lines (Cu II 500.7 nm and Cu II 501.0 nm), are certainly identified. However, although a very strong emission intensity of the copper lines is observed, the emission spectrum suffers from a very high background level. Using the emission intensity at Cu I 521.8 nm and the background level at 527.59 nm, the signal to background (S/B) ratio is approximately 10. The high background level is due to the strong continuous emission inherently occurring during the early regimes of the laser induced plasma formation process, as indicated by the presence of very strong copper ionic emission lines of Cu II 500.7 nm and Cu II 501.0 nm. The two ionic lines are overlapping. In this case, the ratio between the intensity of the atomic emission (Cu I 521.8 nm) and ionic emission (Cu 500.7 nm) is 2.3.

It is considered that immediately after irradiation of the focused laser beam, the laser energy coupled to the sample through multiphoton absorption immediately causes the sample to ablate. The ablated atoms moving at supersonic speed compress the ambient gas in the same manner that a piston compresses fluid, resulting in the generation of a shock wave propagating in the ambient gas. The compression of the ambient gas by the shock front produces a high temperature and high density region, leading to strong ionization confined by the surrounding gas to a very small, localized region slightly above the sample surface [26, 27, 28, 29, 30, 31]. The strong ionization causes the background

emission to occur strongly during the early temporal regimes of the plasma formation process through bremsstrahlung (free–free) and recombination (free–bound) transition mechanisms in the high temperature and high density plasma [32]. At the early stage of the formation process, the high density plasma itself reabsorbs most of the emitted atomic radiation, thus reducing the atomic emission intensity. Thus, the emission spectrum detected in the early regimes is not a true representation of the plasma emission. With time, the initial plasma expands radially into a larger localized region in the ambient gas and then cools, lowering the background level and yielding to a more reliable atomic emission spectrum from the constituents of the irradiated sample and the ambient gas [21, 22, 23, 24, 25, 26, 27, 28, 29, 30, 31, 32]. The plasma temperature was estimated using the following Boltzmann two-line method [32, 33],

$$\frac{I_{ji}^{'}}{I_{ji}} = \left(\frac{\lambda_{ji}}{\lambda_{ji}^{'}}\right)\left(\frac{A_{ji}^{'}}{A_{ji}}\right)\left(\frac{g_{j}^{'}}{g_{j}}\right)\exp\left(\frac{E_{j}^{'} - E_{j}}{kT}\right) \quad (1)$$

where I_{ji}, λ_{ji}, A_{ji}, g_j, and E_j, are the line intensity, transition wavelength, statistical weight, transition possibility, and upper level energy of the spectral line, respectively. k is Boltzmann's constant, and T is the plasma temperature. Furthermore, $I_{ji}^{'}$, $\lambda_{ji}^{'}$, $A_{ji}^{'}$, $g_{j}^{'}$, and $E_{j}^{'}$, are the line intensity, transition wavelength, statistical weight, transition possibility, and upper level energy of another spectral line, respectively [32, 33]. The temperature of the plasma produced under the present experimental parameters of a 54 mJ laser pulse energy, corresponding to a fluency of 27.52 J/cm^2, 760 Torr of surrounding air, and probing the position of the optical fiber just on the plasma center, is approximately 7000 K. These experimental parameters are the typical conditions adopted for LIBS. The high background emission level is basically unfavorable for spectrochemical analysis. Thus, to obtain a spectrochemically useful spectrum using laser induced breakdown spectroscopy (LIBS), a standard OMA system with the capability of a fast temporal gating function is commonly used to avoid the strong continuum emission at the beginning of plasma formation.

Because the compact OMA system operates in free running mode without any gating function, it is not easy to avoid the strong initial background during spectrum acquisition. Considering the emergence process of the continuum emission during plasma formation, obtaining an emission spectrum with features favorable to spectrochemical analysis is assumed to be possible even using the compact OMA system operated in an integrated time mode without any temporal gating function. This result can be achieved by carefully adjusting the crucial experimental parameters. It is well known that plasma formation strongly depends on the energy of the laser pulse coupled to the sample and the density and specific heat of the ambient gas, as related by the Sedov equation. The Sedov formula expresses the movement of the shock front with time as follows [34]:

$$r = \left(\frac{Eo}{\alpha\rho}\right)^{\frac{1}{5}} t^{\frac{2}{5}} \quad (2)$$

where r is the propagation distance of the shock front, t is time measured from the beginning of the explosion, ρ is the gas density, α is a constant involving the specific heat of the gas, and E_0 is the initial explosion energy. This equation explicitly expresses that plasma temporal and spatial behaviors depend on the energy coupled into the sample and on the type and pressure of the ambient gas. Considering this formulation, to obtain better features of the emission spectra using a compact, ungated OMA system, several experimental parameters, including the pressure of the ambient gas, the energy of the laser beam, and the probing position of the optical fiber, were varied.

Figure 2(b) shows the emission spectrum taken from plasma produced on the pure copper sample under an air surrounding at a low pressure of 10 Torr. When the pressure of the ambient air was 10 Torr,

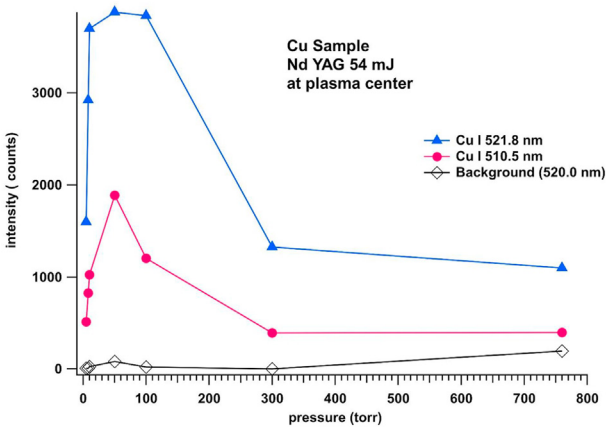

Figure 3. Pressure dependence of the copper atomic emission lines, Cu I 510.5 nm and Cu I 521.8 nm, taken using the compact OMA system under time integration mode.

the features of the emission spectrum were clearly and substantially improved, as shown in Figure 2(b). The signal to background (S/B) ratio is 140, approximately 14-fold better than that of the high pressure case shown Figure 2(a). Similarly, the intensity ratio of the atomic and ionic emission spectra is approximately 13.7, which is approximately 6-fold that of the high pressure case, Figure 2(a). Thus, the background extent and the ionic emission were substantially decreased, confirming the essential role of the ambient gas in the plasma formation process. The background and ionic emission are reduced because the plasma temperature decreases at low pressure because of a weaker confinement of the moving ablated atoms by the lower density ambient gas. The plasma temperature is approximately 8000 K, superficially higher than that in the case of high pressure. However, as mentioned above, the temperature obtained under high pressure and the experimental arrangement is not quite the true temperature of the plasma because the detected emission spectrum strongly suffered from self-absorption. The low pressure emission spectrum indicates that the profile of the emission spectrum detected using a compact OMA system working under the time integration mode can be substantially improved using low pressure regimes of the surrounding gas. For a low cost LIBS system, one might have concern about working at low pressure because the cost of the vacuum pump is high compared to other parts of the LIBS system. In a previous study, a cheap miniature chamber for performing an in situ LIBS experiment was developed [35]. The miniature chamber can be readily evacuated using a small pumping motor. Thus, we expect that a cheap vacuum system for a low cost, low pressure LIBS system can be constructed.

Figure 3 shows a complete plot of the pressure dependence of the copper atomic emission lines, Cu I 510.5 nm and Cu I 521.8 nm, taken using the compact OMA system under a time integration mode. The plasma was produced on the pure copper plate using a laser pulse energy of 54 mJ under ambient air. The emission spectrum was detected by probing the collection optical fiber approximately in the center of the plasma region. Along with the copper atomic emission lines, the background level reading at 520.0 nm was also plotted. The background level increases significantly with pressure because the temperature and density plasma increase with pressure. Notably, the pressure dependence of the emission spectrum obtained using this compact, nongated OMA system is just similar to that of the standard OMA system normally adopted in LIBS. The emission intensity of the copper atomic lines sharply increases at lower pressure regimes, followed by a rapid decay at higher pressures. It is assumed that the sharp increase in the emission intensity under low pressure regimes is due to a larger amount of ablation from the target material compared to the high pressure case due to the optimum reduction of the plasma shielding. As mentioned above, assuming the obeyance of the Boltzmann distribution, the plasma

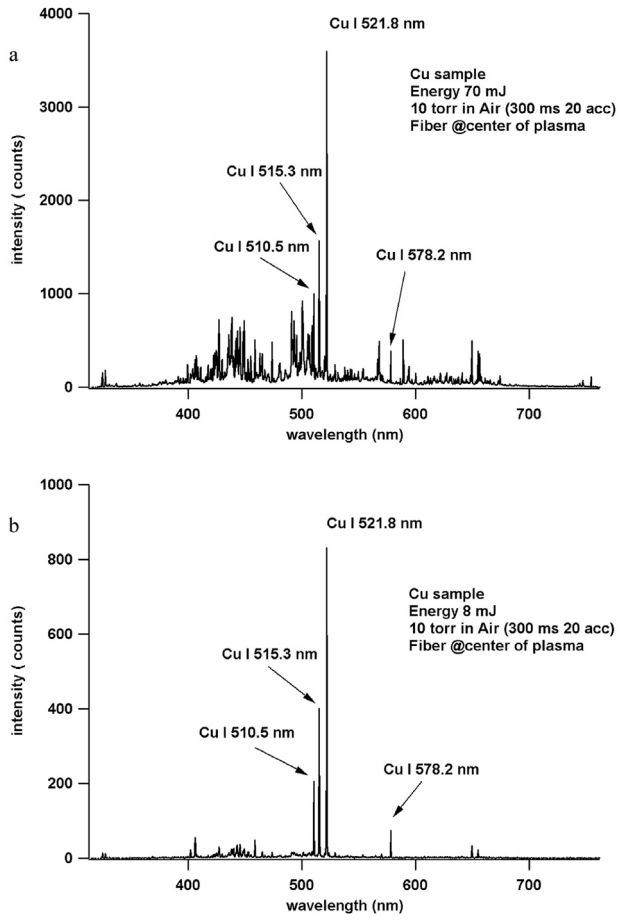

Figure 4. Emission spectrum taken from plasma produced from a pure copper plate under ambient air at a pressure of 10 Torr using a pulse energy of (a) 70 mJ and (b) 8 mJ, respectively.

temperature was estimated using the Boltzmann two-line method. The estimated temperature is relatively high, thus it can excite various elements for performing spectrochemical analysis using the compact, ungated OMA system.

Figure 4(a) exhibits the emission spectrum taken from plasma produced from the pure copper plate under ambient air at a pressure of 10 Torr when the pulse energy was increased to 70 mJ, corresponding to a fluency of 35.67 J/cm^2. In comparison with the 54 mJ case, Figure 2(b), the overall intensity of the emission spectrum greatly increases with energy; however, the background level and ionic emission including noise also increase largely. The copper ionic emission lines, Cu II 500.7 nm and Cu II 501.0 nm, appear clearly along with the copper atomic emission lines of Cu I 510.5 nm, Cu I 515.3 nm, Cu I 521.8 nm, and Cu I 578.2 nm. The signal to background (S/B) ratio of 52.1 is reduced by more than half compared to the 54 mJ case shown Figure 2(b). The atomic to ionic emission intensity ratio is approximately 3.8, which is approximately 3.6 times lower than that of the 54 mJ case, Figure 2(b). The moving speed of the ablating atoms, as expressed by the Sedov equation, increases with the laser energy, thus the higher the laser energy is, the higher the ablating speed will be. The higher speed of the ablating atoms causes a stronger compression with the ambient gas, resulting in a higher temperature and higher density plasma followed by higher continuous and ionic emissions [36, 37, 38, 39, 40]. This result is clearly observed in Figure 4(a); the emission spectrum produced using a higher laser pulse energy exhibits a higher continuum level and higher intensity of ionic emission lines. On the other hand, as displayed in Figure 4(b), when the pulse energy of the laser beam was reduced significantly to a low value of 8 mJ, corresponding to a fluency of 4.08 J/cm^2, the profile of the emission spectrum was remarkably improved, featuring a strong intensity and extremely low background of the copper atomic emission lines, Cu I 510.5 nm, Cu I 515.3 nm, Cu I 521.8 nm, and Cu I 578.2 nm, without any copper ionic emission lines, Cu II 500.7 nm and Cu II 501.0 nm. The signal to background (S/B) ratio is 180.5, a significant increase from the energy cases of 54 mJ and 70 mJ. The atomic to ionic emission intensity ratio is 100.5, a large increase compared to the energy cases of 54 mJ and 70 mJ. When the pulse energy was decreased significantly, in this case from 70 mJ to 8 mJ, the moving speed of the ablated atoms was reduced significantly, weakening the compression with the ambient gas, thus lowering the ionization degree and yielding a very low background and ionic emission, as observed in Figure 4(b). The features of the emission spectrum are favorable for performing qualitative and quantitative analysis. The low energy emission spectrum of plasma under a low pressure surrounding gas using the compact OMA system operated in free running mode is just comparable to that of using the standard OMA system [27, 29].

Considering that immediately after the laser irradiation on the sample surface, there is an initial high temperature and density plasma confined in a small localized region that emerges slightly above the sample surface and is responsible for the high background and ionic emission, another possible strategy to eliminate the high background and ionic emissions when detecting emission spectrum using the compact, ungated OMA system is moving the probing position of the collection optical fiber away from the high temperature and high density plasma region on the sample surface. Figure 5(a), (b), (c), and (d) show the emission spectrum detected from plasma induced on the pure copper plate using the pulse energy of 54 mJ when the probing position of the collection optical fiber was set at 3 mm, 5 mm, 7 mm, and 9 mm above the sample surface, respectively. The plasma was generated under ambient air at a low pressure of 10 Torr. In all these cases, the emission lines due to the copper atom can definitely be observed. However, when the probing position of the optical fiber was set 3 mm above the sample surface, the emission spectrum suffered from a very high background and ionic emission. The signal to background (S/B) ratio is 13.1, and the atomic to ionic emission intensity ratio is 5.4. It is considered that at this probing position, the optical fiber collects emission mostly from the high temperature and high density regions of the plasma slightly above the sample surface. When the probing position of the collection fiber was moved to 5 mm from the sample surface, the total emission obviously increases, but unfortunately the background level and ionic emissions also increase substantially. The signal to background (S/B) ratio is 46.5, which is more than threefold that of the 3 mm case. The atomic to ionic emission intensity ratio is 5.8, very close to that of the 3 mm case. It is understood that at this probing position, the plasma emission from the high temperature and high density plasma region and also from the low temperature and low density plasma region enters the numerical aperture of the collection optical fiber entirely well. However, when the probing position was moved farther away, to 7 mm, the background and ionic emission were greatly diminished. The signal to background (S/B) ratio of 821 is increased considerably compared to those of the 3 mm and 5 mm positions. The atomic to ionic emission intensity ratio of 364.3 is increased tremendously compared to those of the 3 mm and 5 mm positions. The profile of the emission spectrum taken using the compact, ungated OMA system is enhanced incredibly. The copper atomic emission lines, Cu I 510.5 nm, Cu I 515.3 nm, Cu I 521.8 nm, and Cu I 578.2 nm, appear clearly with a very strong intensity, narrow spectral width, and negligible background. Neither of the copper ionic emission lines, Cu II 500.7 nm and Cu II 501.0 nm, appear in the emission spectrum. When the probing position was shifted even farther, to 9 mm above the sample surface, the profile of the emission spectrum was further improved. It is considered that when the probing position was shifted far away, namely, to 7 mm and 9 mm, the emission collected by the optical fiber is mainly from the low temperature and low density plasma region, while the emission from the high temperature and high density plasma localized in a small region slightly above the sample was not significantly coupled into the optical fiber. For

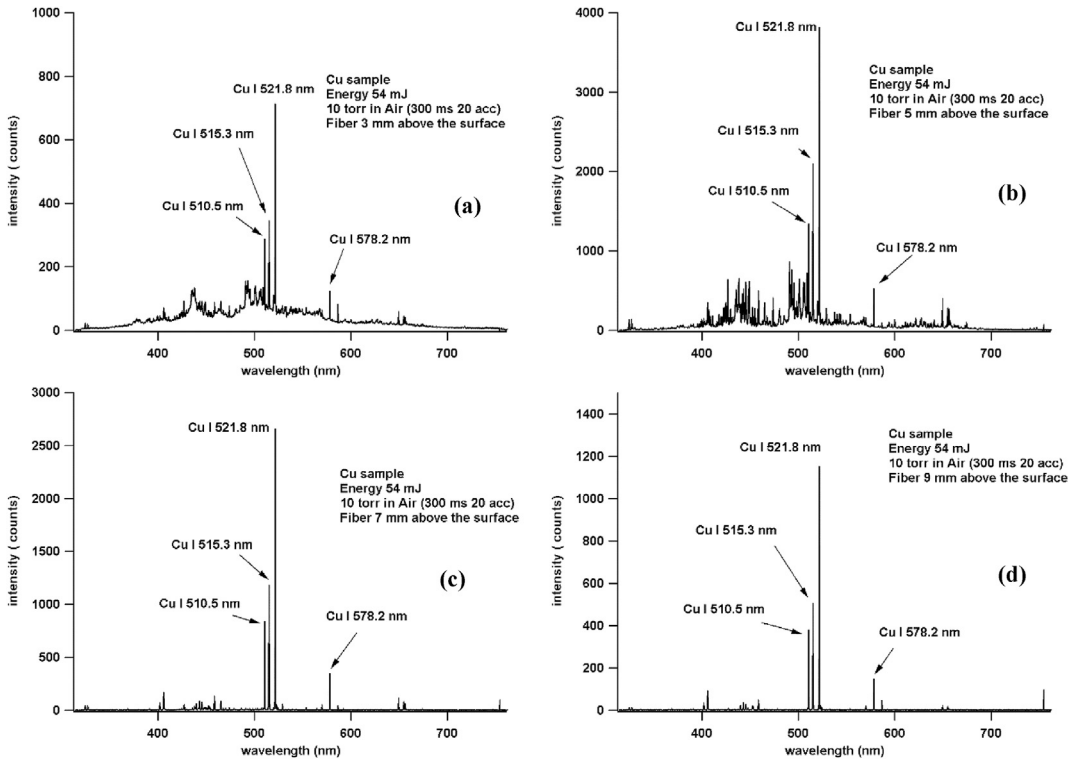

Figure 5. (a), (b), (c), and (d) show the emission spectrum detected from plasma induced on a pure copper plate using a pulse energy of 54 mJ when the probing position of the optical fiber was set at 3 mm, 5 mm, 7 mm, and 9 mm above the sample surface, respectively.

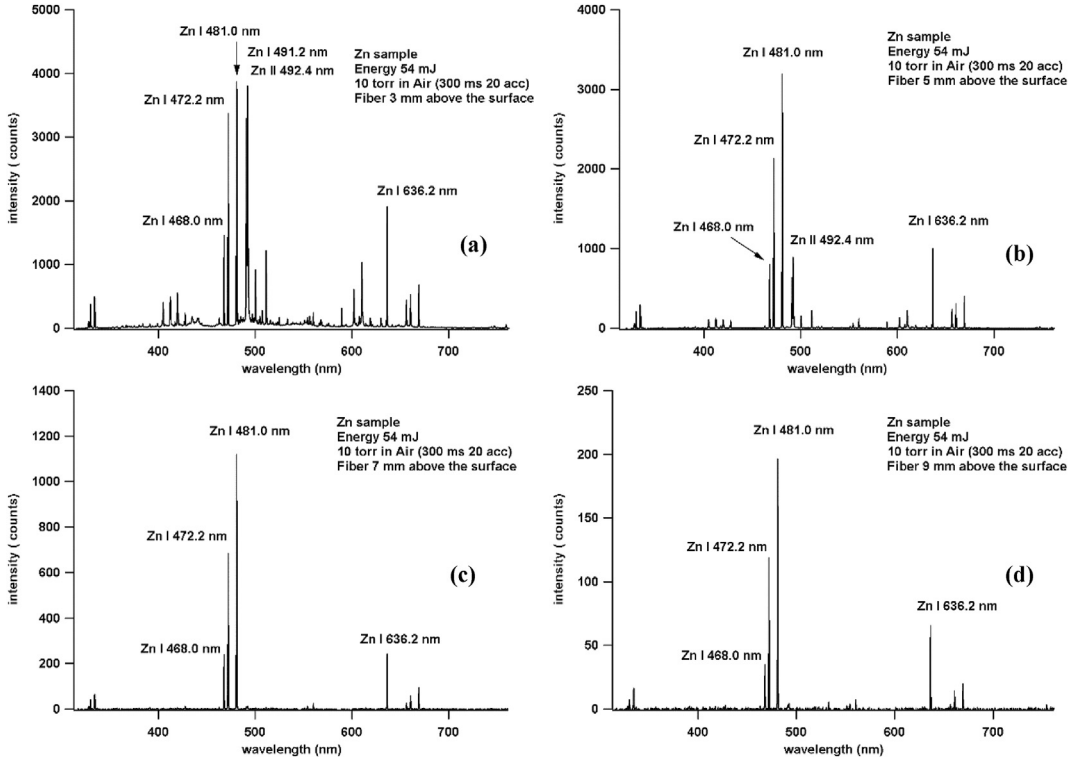

Figure 6. (a), (b), (c), and (d) show the emission spectrum taken from plasma produced on a pure zinc plate using the compact, ungated OMA system detected at different probing positions of the optical fiber above the sample surface, namely, 3 mm, 5 mm, 7 mm, and 9 mm, respectively.

the 9 mm probing position, although the total emission intensity was reduced to approximately half that of the 7 mm case, the copper atomic emission lines, Cu I 510.5 nm, Cu I 515.3 nm, Cu I 521.8 nm, and Cu I 578.2 nm, appear clearly with a negligible background and ionic emission. The signal to background (S/B) ratio of 667.7 was decreased slightly from that of the 7 mm case. The atomic to ionic emission

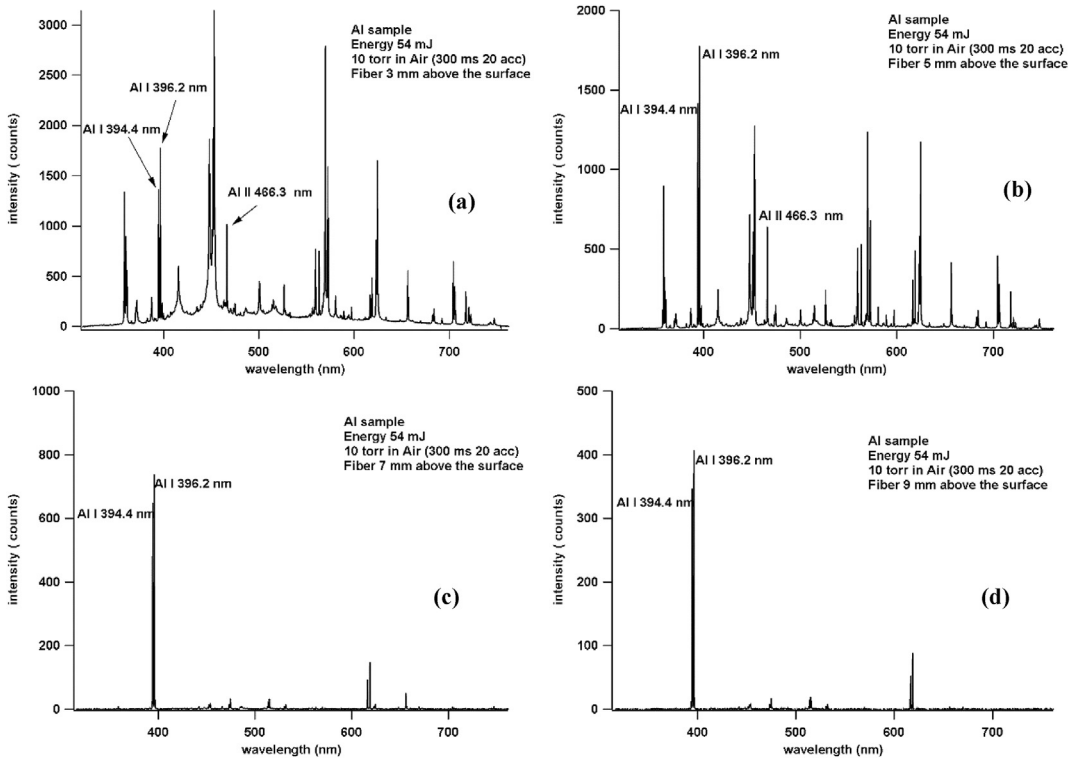

Figure 7. (a), (b), (c), and (d) demonstrate how the emission spectrum taken from a pure aluminum sample changes with the probing position of the optical fiber.

intensity ratio of 404.2 is the highest of all cases, 3 mm, 5 mm, 7 mm, and 9 mm. This emission spectrum taken using the compact, ungated OMA system under such a large integration time at an optical fiber probing position of 9 mm above the sample surface is only similar to that obtained with a standard, gated OMA system and very favorable for spectrochemical analysis, as show in previous works [27, 28, 29, 30].

The influence of the probing position of the optical fiber on the emission spectrum taken using the compact, ungated OMA system under the free running mode was also examined for other samples, namely, pure zinc and pure aluminum plates. Figure 6(a), (b), (c), and (d) show the emission spectrum taken from plasma produced on the pure zinc plate using the compact, ungated OMA system detected at different probing positions of the optical fiber above the sample surface, namely, 3 mm, 5 mm, 7 mm, and 9 mm, respectively. The experiment was conducted using a laser energy of 54 mJ under ambient air at a pressure of 10 Torr. Similar results to those of the copper plate sample were found. For example, at the 3 mm probing position, strong zinc atomic emission lines, namely, Zn I 468.0 nm, Zn I 472.2 nm, Zn I 481.0 nm, and Zn I 636.2 nm, appear together with a high background level and ionic emission (Zn II 492.4 nm). However, the background level and ionic emission then decrease quickly with the increase in the probing position of the optical fiber. An emission spectrum with largely improved features is obtained when the probing position of the collection fiber was 9 mm above the sample surface.

Similar results were obtained for the emission spectrum of the pure aluminum plate sample using the compact, ungated OMA system. Figures 7(a), (b), (c), and (d) demonstrate how the emission spectrum taken from the pure aluminum sample changes with the probing position of the optical fiber. The emission spectrum was detected from a plasma generated on the pure aluminum plate using a laser pulse of 54 mJ under ambient air at a pressure of 10 Torr. Correspondingly, when the plasma emission was detected at the 3 mm probing position, as exhibited in Figure 7(a), strong aluminum atomic emission lines, Al I 394.4 nm and Al I 396.2 nm, were surely detected. However, the emission spectrum suffers from a very high background level and ionic emission, Al II 466.3 nm. As displayed in the consecutive figures, the background and ionic emission decrease quickly with the increase in the probing position of the optical fiber. As shown in Figure 6(d), the optimal profile of the emission spectrum was obtained when the probing position was 9 mm above sample surface, as with the pure copper and zinc plate samples. These results confirm the crucial influence of the probing position of the collection fiber on the features of the emission spectrum detected from the laser induced plasma [20]. These results suggest that the optimum probing position is at a position away from the sample surface.

Notably, a superficial discrepancy is observed in the emission spectra shown in Figure 7, especially between Figure 7(a), Figure 7(b) and Figure 7(c), Figure 7(d). Some emission lines in the emission spectrum displayed in Figure 7(a) and Figure 7(b) are absent from Figure 7(c) and Figure 7(d). This result makes one think that the spectra are for different samples. Actually, these emission lines are second order emission lines

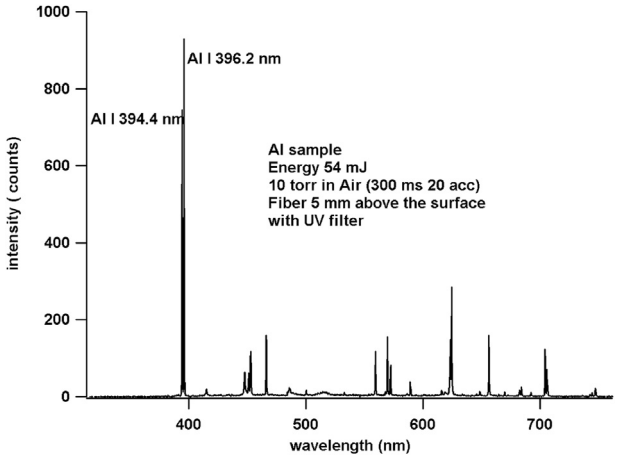

Figure 8. Emission lines due to second order emission in the UV region disappear when a UV filter was set in front of the optical fiber during detection of the emission spectrum.

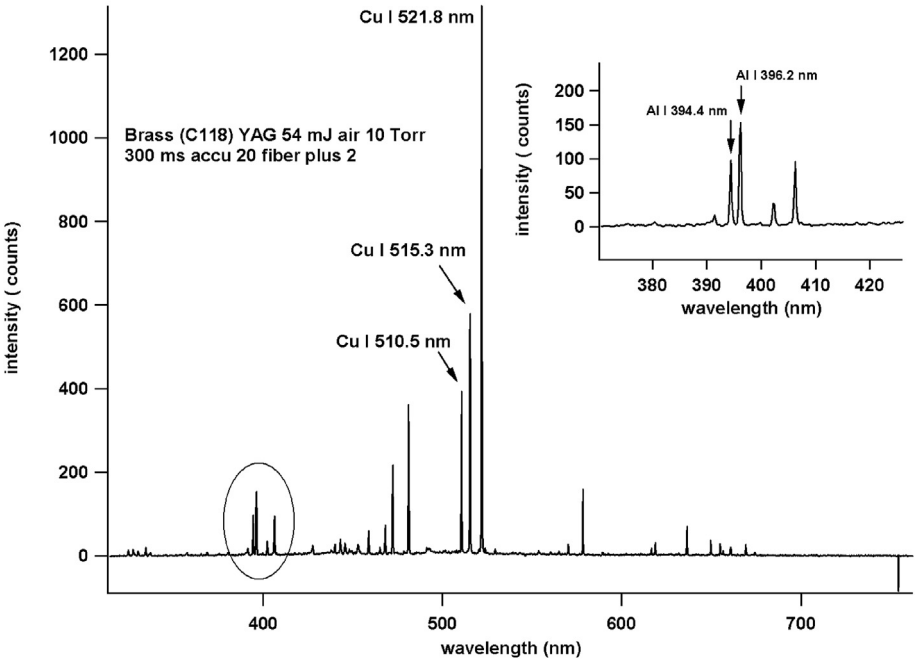

Figure 9. Emission spectrum taken from a brass standard sample (C118) containing aluminum as an impurity.

occurring in the ultraviolet (UV) region and are neither atomic nor ionic aluminum emission lines. To confirm this explanation, a UV filter was used during acquisition of the emission spectrum. As presented in Figure 8, the second order emission lines in the UV region disappeared when a UV filter was set in front of the optical fiber during detection of the emission spectrum. This result confirms that the emission lines are due to aluminum, as shown in Figure 7(c) and (d).

After inspecting the dependence of the features of the emission spectra taken using the compact, ungated OMA system on the experimental configurations, namely, the energy of the laser pulse, the pressure of the surrounding gas, and the position of the probing optical fiber, and determining the optimum experimental conditions, LIBS using the compact, ungated OMA system was applied to a semiquantitative practical analysis. Figure 9 shows the emission spectrum taken from a brass standard sample (C1118) containing aluminum at a concentration of 2.80%. This standard alloy contains Cu (75.1%) and Zn (21,9%) as the major constituents, and the minor and trace elements include Al, Fe, Pb, and Si. The plasma was produced using a laser pulse of 54 mJ under air as the surrounding gas at a pressure of 10 Torr. The integration time of the detector of the compact, ungated OMA system was set for 300 ms with 20 accumulations. The probing position of the optical fiber was set at 2 mm above the sample surface. The aluminum atomic emission lines, Al I 364.4 nm and Al I 396.2 nm, along with the strong, typical copper emission lines of Cu I 510.5 nm, Cu I 515.3 nm, Cu I 521.8 nm, and Cu I 578.2 nm, are clearly apparent. The limit of detection under the current

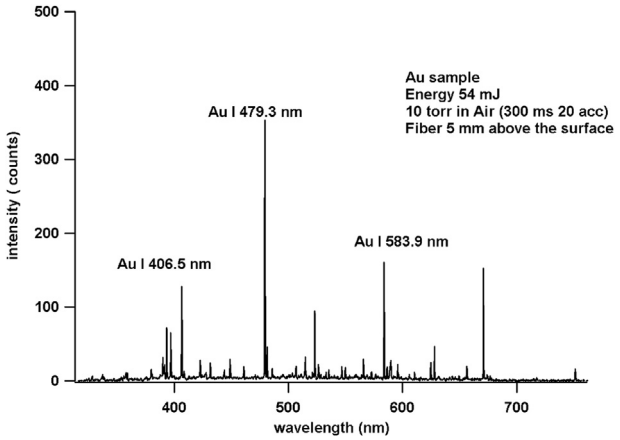

Figure 10. Emission spectrum taken from plasma produced on a gold sample using a Nd-YAG laser of 54 mJ under air at a pressure of 10 Torr.

(a)

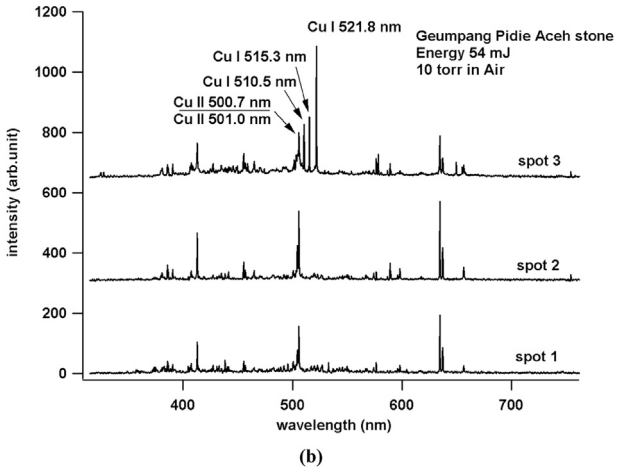

(b)

Figure 11. (a) Photo of a natural stone sample collected from a traditional mining site in the Geumpang region, Pidie Regency, Aceh, Indonesia; and (b) emission spectra detected from different spots on the natural stone sample.

experimental conditions for aluminum in the brass standard sample is roughly 0.18%.

In addition to the brass standard sample, a commercial gold sample claimed to be of high purity was purchased from an ordinary shop and spectrally analyzed using LIBS with the compact, ungated OMA system under optimized experimental conditions. Figure 10 shows the emission spectrum taken from the plasma produced on the gold sample using a Nd-YAG laser of 54 mJ under air at a pressure of 10 Torr. The probing position of the collection optical fiber was set at 5 mm above the sample surface. It is clearly apparent that there are many strong emission lines due to gold, namely, Au I 406.5 nm, Au I 479.3 nm, and Au I 583.9 nm. However, unfortunately, the spectrum is actually not purely due to gold, as abandoned emission lines due to impurities appear in the spectrum along with Au emission lines, refuting the high purity claim made by its sellers.

Next, the compact, ungated OMA system was applied to analyzing a natural stone collected from a traditional gold mining site in the Geumpang region located in Pidie Regency, which is a part of the Aceh prefecture in Indonesia. These traditional miners do not have access to well established analytical tools because of limited funds and knowledge. Based on direct visual observations, many spots on the surface of the natural stone glitter, thus traditional miners believe that the natural stone contains gold, as displayed in Figure 11(a). This superficial assumption results in an increase in the price of the natural stone. However, a measurement using the ungated, compact OMA system, as shown in Figure 11(b), clearly revealed the falsity of this conjecture. The emission spectra were taken from different spots on the stone surface, namely, the glittering spot of 3 and the unglittering, normal spots of 1 and 2. Strong copper emission lines, namely, the atomic lines of Cu I 510.5 nm, Cu I 515.3 nm, Cu I 521.8 nm, and Cu I 578.2 nm, together with the ionic emission lines of Cu II 500.7 nm and Cu II 501.0 nm, were undoubtedly detected from the glittering spot (spot 3), whereas they were absent from the spectra of the unglittering spots (spot 1 and spot 2). This result confirmed that the glittering occurs because of the presence of copper, not because of gold content.

4. Conclusion

Characteristics of laser induced plasma can be studied systematically using an ungated, compact OMA system under a time integrated mode. By optimizing several experimental parameters, including the pressure of the ambient gas, the energy of the laser pulse, and the probing position of the optical fibers, quality emission spectra with features favorable for spectrochemical analysis can be obtained using the compact OMA system, just similar to those obtained using a sophisticated, precisely temporal gated OMA system. The optimum condition was achieved at a low ambient gas pressure of 10 Torr, a low energy laser pulse of 8 mJ, and a probing position of the collection optical fibers of more than 5 mm from the sample surface. The LIBS with the ungated, compact OMA system under the optimum condition was used for preliminary practical applications, namely, inspection of the standard brass alloy and commercial high purity gold. It was also applied to studying geological samples of a natural mining stone, confirming the eventuality of the LIBS with a compact, ungated OMA system for quick, practical analysis.

Declarations

Author contribution statement

Nasrullah Idris: Conceived and designed the experiments; Analyzed and interpreted the data; Wrote the paper.

Kurnia Lahna, Maria Margareta Suliyanti: Performed the experiments.

Muliadi Ramli: Performed the experiments; Contributed reagents, materials, analysis tools or data.

Taufik Fuadi Abidin, Wahyu Setia Budi: Analyzed and interpreted the data.

Koo Hendrik Kurniawan: Conceived and designed the experiments; Contributed reagents, materials, analysis tools or data.

May On Tjia: Conceived and designed the experiments.

Kiichiro Kagawa: Conceived and designed the experiments; Analyzed and interpreted the data.

Funding statement

Nasrullah Idris was supported by Kementerian Riset Teknologi dan Pendidikan Tinggi Republik Indonesia (215/SP2H/LT/DPRM/2019) and Universitas Syiah Kuala (ID) (523/UN11/SPK/PNBP/2019). Koo Hendrik Kurniawan was supported by The Academy of Sciences for the Developing World, Third World Academy of Sciences (TWAS) (060150 RG/PHYS/AS/UNESCO FR:3240144882).

Declaration of interests statement

The authors declare no conflict of interest.

Additional information

No additional information is available for this paper.

References

[1] J.D. Winefordner, I.B. Gornushkin, T. Correll, E. Gibb, B.W. Smith, N. Omenetto, Comparing several atomic spectrometric methods to the super stars: special issue on laser-induced breakdown spectrometry, LIBS, a future super star, J. Anal. Atomic Spectrom. 19 (2004) 106–108.

[2] D.W. Hahn, N. Omenetto, Laser-induced breakdown spectroscopy (LIBS), Part I: review of basic diagnostics and plasma–particle interactions: still-challenging issues within the, Anal. Plasma Commun. Appl. Spectrosc. 64 (12) (2010) 335A–366A.

[3] D.W. Hahn, N. Omenetto, Laser-induced breakdown spectroscopy (LIBS), Part II: review of instrumental and methodological approaches to material analysis and applications to different fields, Appl. Spectrosc. 66 (4) (2012) 347–419.

[4] B.C. Castle, A.K. Knight, K. Visser, B.W. Smith, J.D. Winefordner, Battery powered laser-induced plasma spectrometer for elemental determinations, J. Anal. At. Spectrom. 13 (1998) 589–595.

[5] I.B. Gornushkin, B.W. Smith, H. Nasajpour, J.D. Winefordner, Identification of solid materials by correlation analysis using a microscopic laser-induced plasma spectrometer, Anal. Chem. 71 (1999) 5157–5164.

[6] G. Galbacs, I.B. Gornushkin, B.W. Smith, J.D. Winefordner, Semi quantitative analysis of binary alloys using laser-induced breakdown spectroscopy and a new calibration approach based on linear correlation Spectrochim, Acta Bot. 56 (2001) 1159–1173.

[7] A. Jabbar, M. Akhtar, S. Mehmmod, M. Iqbal, R. Ahmed, M.A. Baig, Quantification of copper remediation in the Allium cepa L. leaves using electric field assisted laser induced breakdown spectroscopy Spectrochim, Acta Part B 162 (2019) 105719.

[8] M. Akhtar, A. Jabbar, N. Ahmed, S. Mahmood, Z.A. Umar, R. Ahmed, M.A. Baig, Analysis of lead and copper in soil samples by laser-induced breakdown spectroscopy under external magnetic field, Appl. Phys. B 125 (2019) 110.

[9] N. Ahmed, R. Ahmed, M. Rafiqe, M.A. Baig, A Comparative Study of Cu-Ni Alloy Using LIBS, LA-TOF, EDX, and XRF Laser and Particle Beams, 16, Cambridge University Press, 2016, pp. 1–9.

[10] T.J. Lie, K.H. Kurniawan, D.P. Kurniawan, M. Pardede, M.M. Suliyanti, A. Khumaeni, S.A. Natiq, S.N. Abdulmadjid, Y.I. Lee, K. Kagawa, N. Idris, M.O. Tjia, Elemental analysis of bead samples using a laser-induced plasma at low pressure Spectrochim, Acta Part B 61 (1) (2006) 104–112.

[11] K.M. Abedin, A.F.M.Y. Haider, M.A. Rony, Z.H. Khan, Identification of multiple rare earths and associated elements in raw monazite sands by laser-induced breakdown spectroscopy, Optic Laser. Technol. 43 (1) (2011) 45–49.

[12] J. Li, J. Lu, Z. Lin, S. Gong, C. Xi, L. Chang, L. Yang, P. Li, Effects of experimental parameters on elemental analysis of coal by laser-induced breakdown spectroscopy, Optic Laser. Technol. 41 (8) (2009) 907–913.

[13] B. Salle, D.A. Cremers, S. Maurice, R.C. Wiens, P. Fichet, Evaluation of a compact spectrograph for in-situ and stand-off Laser-Induced Breakdown Spectroscopy analyses of geological samples on Mars missions Spectrochim, Acta Part B 60 (2005) 805–815.

[14] L. Qing-Yu, D. Yi-Xiang, Laser-induced breakdown spectroscopy: from experimental platform to field instrument chin, J. Anal. Chem. 45 (9) (2017) 1405–1414.

[15] J. Goujon, A. Giakoumaki, V. Piñon, O. Musset, D. Anglos, E. Georgiou, J.P. Boquillon, A compact and portable laser-induced breakdown spectroscopy instrument for single and double pulse applications Spectrochim, Acta Part B 63 (2008) 1091–1096.

[16] R. Junjuri, A.K. Myakalwar, M.K. Gundawar, Standoff detection of explosives at 1 m using laser induced breakdown spectroscopy, Defence Sci. J. 67 (6) (2017) 623–630.
[17] M.M. Tamboli, V.K. Unnikrishnan, R. Nayak, P. Devangad, K.M. Muhammed Shameem, V.B. Kartha, C. Santhosh, Development of a stand-off laser induced breakdown spectroscopy (ST-LIBS) system for the analysis of complex matrices, J. Instrum. 11 (98) (2016) P08021.
[18] D.A. Cremers, R.C. Chinni, Laser-induced breakdown spectroscopy—capabilities and limitations, Appl. Spectrosc. Rev. 44 (2009) 457–506.
[19] J.L. Gottfried, F.C. De Lucia Jr., Laser-Induced Breakdown Spectroscopy: Capabilities and Applications, Army Research Laboratory, 2010, pp. 1–24.
[20] V. Motto-Ros, E. Negre, F. Pelascini, G. Panczer, J. Yu, Precise alignment of the collection fiber assisted by real-time plasma imaging in laser-induced breakdown spectroscopy", Spectrochim. Acta, Part B 92 (2014) 60–69.
[21] J. Cortez, B.B.F. Filho, L.M. Fontes, C. Pasquini, I.M. Raimundo Jr., M.F. Pimentel, F. de Souza Lins Borba, A simple device for lens-to-sample distance adjustment in laser-induced breakdown spectroscopy (LIBS), Appl. Spectrosc. 71 (4) (2017) 634–639.
[22] H. Kim, Y. Jeon, W.B. Lee, S.H. Nam, S.H. Han, K.S. Ham, V.S. Singh, Y. Lee, Feasibility of quantitative analysis of magnesium and calcium in edible salts using a simple laser-induced breakdown spectroscopy device, Appl. Spectrosc. 73 (10) (2019) 1172–1182.
[23] C. Lopez-Moreno, K. Amponsah-Manager, B.W. Smith, I.B. Gornushkin, N. Omenetto, S. Palanco, J.J. Laserna, J.D. Winefordner, Quantitative analysis of low-alloy steel by microchip laser induced breakdown spectroscopy, J. Anal. At. Spectrom. 20 (6) (2005) 552–556.
[24] M.S. Afgan, Z. Hou, Z. Wang, Quantitative analysis of common elements in steel using a handheld-LIBS instrument, J. Anal. At. Spectrom. 32 (10) (2017) 1905–1915.
[25] F.B. Gonzaga, C. Pasquini, A compact and low cost laser induced breakdown spectroscopic system: application for simultaneous determination of chromium and nickel in steel using multivariate calibration Spectrochim, Acta Part B 69 (2012) 20–24.
[26] M.M. Suliyanti, Isnaeni, M. Pardede, I. Karnadi, I. Tanra, J. Iqbal, M. Bilal, M.A. Marpaung, R. Hedwig, Z.S. Lie, M. Ramli, S.N. Abdulmadjid, N. Idris, A. Khumaeni, K.H. Kurniawan, K. Kagawa, M.O. Tjia, Comparison of excitation mechanisms and the corresponding emission spectra in femto second and nano second laser-induced breakdown spectroscopy in reduced ambient air and their performances in surface analysis, J. Laser Appl. 32 (1) (2020), 012014.
[27] N. Idris, M. Pardede, E. Jobiliong, Z.S. Lie, R. Hedwig, M.M. Suliyanti, D.P. Kurniawan, K.H. Kurniawan, K. Kagawa, M.O. Tjia, Enhancement of carbon detection sensitivity in laser induced breakdown spectroscopy with low pressure ambient helium gas Spectrochim, Acta Part B 161 (2019) 26–32.
[28] N. Idris, M. Pardede, K.H. Kurniawan, K. Kagawa, M.O. Tjia, Shock wave plasma induced emission generated by low energy nanosecond Nd: YAG laser in open air and its application to quantitative Cr analysis of low alloy steel, AIP Adv. 8 (5) (2018) 55121.
[29] J. Iqbal, M. Pardede, E. Jobiliong, R. Hedwig, M. Ramli, A. Khumaeni, W.S. Budi, N. Idris, S.N. Abdulmadjid, K. Lahna, M.A. Marpaung, I. Karnadi, Z.S. Lie, H. Suyanto, D.P. Kurniawan, T.J. Lie, K.H. Kurniawan, K. Kagawa, M.O. Tjia, Shock wave plasma generation in low pressure ambient gas from powder sample using subtarget supported micro mesh as a sample holder and its potential applications for sensitive analysis of powder samples Microchem, J 142 (2018) 108–116.
[30] N. Idris, K. Lahna, S.N. Abdulmadjid, M. Ramli, H. Suyanto, A.M. Marpaung, M. Pardede, E. Jobiliong, R. Hedwig, M.M. Suliyanti, Z.S. Lie, T.J. Lie, K. Kagawa, M.O. Tjia, K.H. Kurniawan, Excitation mechanisms in 1 mJ picosecond laser induced low pressure He plasma and the resulting spectral quality enhancement, J. Appl. Phys. 117 (22) (2015) 223301.
[31] W.S. Budi, H. Suyanto, K.H. Kurniawan, M.O. Tjia, K. Kagawa, Shock excitation and cooling stage in the laser plasma induced by a Q-switched Nd:YAG laser at low pressures, Appl. Spectrosc. 53 (6) (1999) 719–730.
[32] D.A. Cremers, L.J. Radziemski, Handbook of Laser-Induced Breakdown Spectroscopy, John Wiley and Sons, Ltd, England, 2006.
[33] S. Zhang, X. Wang, M. He, Y. Jiang, B. Zhang, W. Hang, B huang laser-induced plasma, Temp. Spectrochim. Acta Part B 97 (2014) 13–33.
[34] L.I. Sedov, Similarity and Dimensional Methods in Mechanics, Mir Publishers, Moscow, 1982.
[35] T.J. Lie, H. Kurniawan, R. Hedwig, M. Pardede, M.O. Tjia, N. Idris, T. Kobayashi, Y.I. Lee, K. Kagawa, Low pressure plasma confined in a miniature cylindrical chamber and its application for in-situ elemental analysis Jpn, J. Appl. Phys. 44 (1A) (2005) 202.
[36] K. Tsuyuki, S. Miura, N. Idris, K.H. Kurniawan, T.J. Lie, K. Kagawa, Measurement of concrete strength using the emission intensity ratio between Ca (II) 396.8 nm and Ca (I) 422.6 nm in a Nd: YAG laser-induced plasma, Appl. Spectrosc. 60 (1) (2006) 61–64.
[37] S.N. Abdulmadjid, M. Pardede, H. Suyanto, M. Ramli, K. Lahna, A.M. Marpaung, R. Hedwig, Z.S. Lie, D.P. Kurniawan, K.H. Kurniawan, T.J. Lie, N. Idris, M.O. Tjia, K. Kagawa, Evidence of feasible hardness test on Mars using ratio of ionic/neutral emission intensities measured with laser-induced breakdown spectroscopy in low pressure CO2 ambient gas, J. Appl. Phys. 119 (16) (2016) 163304.
[38] Z.A. Abdel-Salam, Z. Nanjing, D. Anglos, M.A. Harith, Effect of experimental conditions on surface hardness measurements of calcified tissues via LIBS, Appl. Phys. B 94 (1) (2009) 141–147.
[39] Z.A. Abdel-Salam, A.H. Galmed, E. Tognoni, M.A. Harith, Estimation of calcified tissues hardness via calcium and magnesium ionic to atomic line intensity ratio in laser induced breakdown spectra Spectrochim, Acta Part B 62 (12) (2007) 1343–1347.
[40] H. Kurniawan, T.J. Lie, N. Idris, M.O. Tjia, M. Ueda, K. Kagawa, Detection of the density jump in the laser-induced shock wave plasma using low energy Nd: YAG laser at low pressures of air, J. Spectrosc. Soc. Jpn. 50 (1) (2001) 13–18.